Contribution from the Department of Chemistry,
University of Otago, Dunedin, New Zealand

Importance of Ion Association in the Induced Reactions of Cobalt(III)–Acido Complexes. 3.[1] Hg^{2+}- and Ag^{+}-Catalyzed Reactions of the *t*-$[Co(tren)(NH_3)SCN]^{2+}$ Ion

David A. Buckingham,* Charles R. Clark, and Margot J. Gaudin

Received May 21, 1987

The Hg^{2+}-induced reaction of *t*-$[Co(tren)(NH_3)SCN]^{2+}$ (hereafter $CoSCN^{2+}$) in the presence and absence of added anions Y^- (NO_3^-, ClO_4^-, $CF_3SO_3^-$) has been studied kinetically (spectrophotometric) and studied as reaction products (RP-HPIPC data). The kinetic data with varying $[Hg^{2+}]$ (0.04–0.40 mol dm^{-3}) and Y_1^- and Y_2^- mixtures ($[Y_1^-] + [Y_2^-] = 1.00$ mol dm^{-3}) fit the rate expression $k_{obsd} = (k_0K^0_{Co} + k_1K^1_{Co}K^1_{Hg}[Y_1^-] + k_2K^2_{Co}K^2_{Hg}[Y_2^-])[Hg^{2+}]/(1 + K^1_{Hg}[Y_1^-] + K^2_{Hg}[Y_2^-] + (K^0_{Co} + K^1_{Co}K^1_{Hg}[Y_1^-] + K^2_{Co}K^2_{Hg}[Y_2^-])[Hg^{2+}])$ whereas at $[Hg^{2+}] = 0.04$ mol dm^{-3} and in the presence of a single Y^- (0.10–1.36 mol dm^{-3}) the data fit the simpler expression $k_{obsd} = (k_0K^0_{Co} + k_1K_{Co}K_{Hg}[Y^-])[Hg^{2+}]$. At 25.0 °C $k_0K^0_{Co}$ takes the value 4.3×10^{-3} mol^{-1} dm^3 s^{-1}, $K_{Co}K_{Hg}$ the values 2.2 ± 0.3 (NO_3^-), 0.9 ± 0.2 (ClO_4^-), and 0.6 ± 0.1 ($CF_3SO_3^-$) mol^{-2} dm^6, and k_1 the values $(3.9 \pm 0.5) \times 10^{-2}$ (NO_3^-), $(3.5 \pm 0.5) \times 10^{-2}$ (ClO_4^-), and $(2.6 \pm 0.5) \times 10^{-2}$ ($CF_3SO_3^-$) s^{-1}. The reaction is interpreted in terms of equilibrium attachment of Hg^{2+} (K^0_{Co}), or HgY^+ ($K_{Co}K_{Hg}$), to the sulfur atom of coordinated thiocyanate followed by rate-determining cleavage of the Co–SCN bond (k_0, k_1). The k_0 pathway results in 58% $CoNCS^{2+}$ and 42% $CoOH_2^{3+}$ products, the k_1 pathway ($Y^- = NO_3^-$) results in 23% $CoNCS^{2+}$, 22% $CoOH_2^{3+}$, and 55% $CoONO_2^{2+}$, and the k_1 pathways ($Y^- = ClO_4^-$, $CF_3SO_3^-$) ultimately result in 40% $CoNCS^{2+}$ and 60% $CoOH_2^{3+}$ although some $CoOClO_3^{2+}$ and $CoOSO_2CF_3^{2+}$ are likely as intermediates. The ability of Y^- to compete for both the $CoNCS^{2+}$ and $CoOH_2^{3+}$ products is interpreted in terms of competition at the reaction site following cleavage of the Co–SCN bond. The Ag^+-induced reaction of $CoSCN^{2+}$ fits the rate expression $k_{obsd} = (k_1K^1_{Ag}[Ag^+] + k_2K^1_{Ag}K^2_{Ag}[Ag^+]^2)/(1 + K^1_{Ag}[Ag^+])$ in 1.00 mol dm^{-3} ClO_4^- with k_1, K^1_{Ag}, and $k_2K^2_{Ag}$ taking the values 3.4 $\times 10^{-4}$ s^{-1}, 1.0 mol^{-1} dm^3, and 6.8×10^{-4} mol^{-1} dm^3 s^{-1}, respectively, at 25.0 °C. The k_1 pathway results in 80% $CoNCS^{2+}$ and 20% $CoOH_2^{3+}$ products and the k_2 reaction in ~100% $CoOH_2^{3+}$. Replacement of ClO_4^- by NO_3^- accelerates the rate and results in a limiting distribution of products (10% $CoNCS^{2+}$, 29% $CoOH_2^{3+}$, 61% $CoONO_2^{2+}$) at 1.00 mol dm^{-3} NO_3^- for $[Ag^+] = 1.00$ mol dm^{-3}. The rate and product data are interpreted in terms of the binding of Ag^+ ions to both the S and N ends of coordinated thiocyanate followed by Co–SCN^{2+} bond cleavage and competition by NCS^-, OH_2, and Y^- (ClO_4^-, NO_3^-) for the intermediate of reduced coordination number.

Introduction

For several years we have been interested in the lifetimes of intermediates of reduced coordination number produced during the substitution reactions of Co(III)–acido complexes. As more information becomes available the less sure we are that such an intermediate exists for sufficient time to have a chemistry of its own. Prior events in the substitution process appear to control its fate. For example, in the induced reaction $Co(NH_3)_5N_3^{2+}$ + NOX the evidence now suggests that incorporation of Y^- (e.g. NO_3^-, Cl^-) into the products of this very rapid process probably arises from preassociation in the reactant $Co(NH_3)_5N_3^{2+}$ complex (i.e. as $Y^-{\cdot}Co(NH_3)_5N_3^{2+}$)[1] rather than by diffusion of Y^- from the bulk solution to a stabilized $Co(NH_3)_5N_2O^{3+}$ or $Co(NH_3)_5^{3+}$ intermediate.[2]

Some 10 years ago Adegite, Orhanovic, and Sutin showed[3] that the induced reaction $Co(NH_3)_5SCN^{2+} + Hg^{2+}$ produced a substantial amount of $Co(NH_3)_5NCS^{2+}$ in addition to $Co(NH_3)_5OH_2^{3+}$ (a close to 50:50 product distribution was found). They discussed this in terms of solvent cage effects in which bond rotation and reentry of NCS^- into the coordination sphere competed for the complete escape of $HgSCN^+$ and entry of OH_2.[2,2] This paper explores the similar reaction of *t*-$[Co(tren)(NH_3)SCN]^{2+}$ in detail by using another anion Y^- to compete for the bound rotation process. The formation of substantial amounts of CoY^{2+} product in addition to $CoNCS^{2+}$ requires a close association between the two entering groups at the point of entry, and this is discussed in terms of Y^- being present in the activated complex for breaking of the Co–SCN bond. The results obtained are compared with those for other induced reactions.

Results

In what follows the *t*-$Co(tren)(NH_3)^{3+}$ moiety is represented by Co, and the products derived from both the Hg^{2+}- and Ag^+-induced reactions have the *t*-configuration.

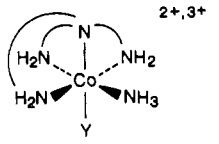

1. Kinetic Data. (a) Hg^{2+}-Catalyzed Reaction. Three sets of spectrophotometric rate data were collected at 550 nm where the absorbance change is maximized (≈0.1 OD units, $[Co]_T \approx 2 \times 10^{-3}$ mol dm^{-3}). Good first-order traces were obtained over 3–4 reaction half-lives. The first set of data, Figure 1, relates to a constant $[Hg^{2+}] = 0.04$ mol dm^{-3}, constant [HY] = 0.02 mol dm^{-3}, and varying $[Y^-] = 0.1$–1.36 mol dm^{-3}. The ionic strength varies from 0.14 to 1.40 mol dm^{-3} for these solutions. The figure shows linear correlations between k_{obsd} and $[Y^-]$ for each of the anions NO_3^-, ClO_4^-, and $CF_3SO_3^-$ with a common nonzero intercept. Thus $k_{obsd} = k^1_0 + k^1_Y[Y^-]$ with $k^1_0 = (1.7 \pm 0.2) \times 10^{-4}$ s^{-1}, $k^1_Y = 28.5 \times 10^{-4}$ mol^{-1} dm^3 s^{-1} (NO_3^-), 11.1×10^{-4} mol^{-1} dm^3 s^{-1} (ClO_4^-), and 5.6×10^{-4} mol^{-1} dm^3 s^{-1} ($CF_3SO_3^-$) at 25.0 °C.

The second set of data, Figure 2, corresponds to a constant $[Y^-] = 1.00$ mol dm^{-3} and constant [HY] = 0.20 mol dm^{-3} but varying $[Hg]_T = 0.04$–0.40 mol dm^{-3}. Because $[Y^-]$ was made up with NaY, the ionic strength for these solutions varies somewhat, 1.04–1.40 mol dm^{-3}. Figure 3 shows a similar set of data for NO_3^- and ClO_4^- at a constant ionic strength of 1.40 mol dm^{-3}. This involves variable $[Y^-] = 1.36$–1.00 mol dm^{-3}. Both sets of data show curvature in the plots of k_{obsd} vs $[Hg]_T$ with that for Figure 3 being somewhat more pronounced than that for Figure 2.

The third set of data was obtained by using mixed NO_3^- and $CF_3SO_3^-$ solutions such that $[NO_3^-] + [CF_3SO_3^-] = 1.00$ mol dm^{-3} but with varying concentrations of each, 0–1.00 mol dm^{-3}. Figure 4 gives this data at three Hg^{2+} concentrations: 0.04 mol dm^3 ($[H^+] = 0.02$ mol dm^{-3}, $I = 1.04$ mol dm^{-3}), 0.20 ($[H^+] = 0.10$, $I = 1.20$), and 0.40 ($[H^+] = 0.20$, $I = 1.40$). Curvature in these plots becomes increasingly apparent with increasing $[Hg]_T$.

(b) Ag^+-Catalyzed Reaction. Rates were obtained by following the decrease in the amount of $CoSCN^{2+}$ as a function of time with RP-HPIPC analysis. Direct spectrophotometric determination

(1) Part 2: Buckingham, D. A.; Clark, C. R.; Webley, W. S. *Inorg. Chem.* **1982**, *21*, 3353.
(2) Haim, A.; Taube, H. *Inorg. Chem.* **1963**, *2*, 1199.
(3) Adegite, A.; Orhanovic, M.; Sutin, N. *Inorg. Chim. Acta* **1975**, *15*, 185.
(4) James, D. W. *Prog. Inorg. Chem.* **1985**, *33*, 353.

0020-1669/88/1327-0293$01.50/0

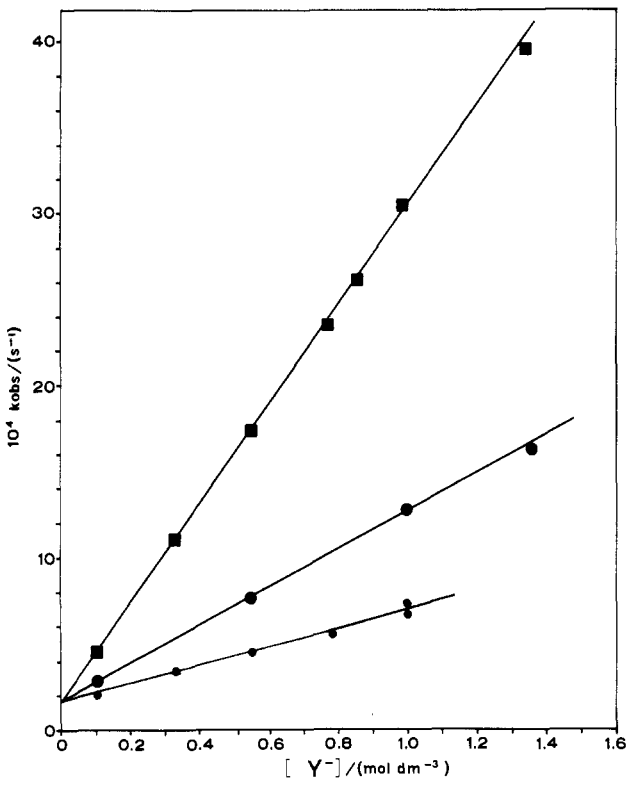

Figure 1. Variation in k_{obsd} with $[Y^-]$ (0.1–1.36 mol dm^{-3}) at $[Hg^{2+}]$ = 0.04 mol dm^{-3}, $[H^+]$ = 0.02 mol dm^{-3}, λ = 550 nm, and 25.0 °C: (■) NO_3^-; (●) ClO_4^-; (•) $CF_3SO_3^-$. The full lines are drawn by using (5a) and constants given in the text.

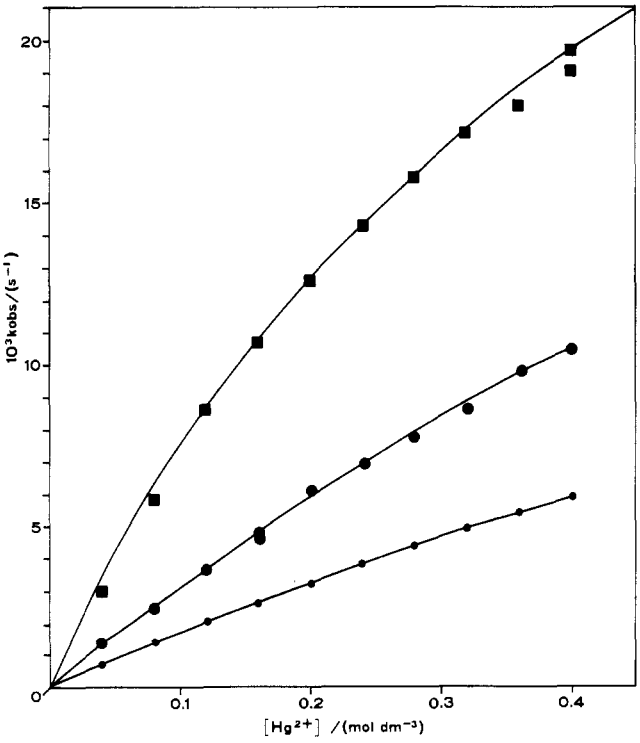

Figure 2. Variation in k_{obsd} with $[Hg^{2+}]$ (0.04–0.40 mol dm^{-3}) at constant $[Y^-]$ = 1.00 mol dm^{-3}, I = 1.04–1.40 mol dm^{-3}, constant $[H^+]$ = 0.20 mol dm^{-3}, λ = 550 nm, and 25.0 °C: (■) NO_3^-; (●) ClO_4^-; (•) $CF_3SO_3^-$.

is not possible in this case since AgSCN gradually precipitates. The RP-HPIPC method also has the advantage of giving a complete survey of the products and reactants as a function of time. The sequence of chromatograms given by Figure 5 shows the quality of the data, and once set up (in terms of column equilibration, injection volume, and solvent program) this method is

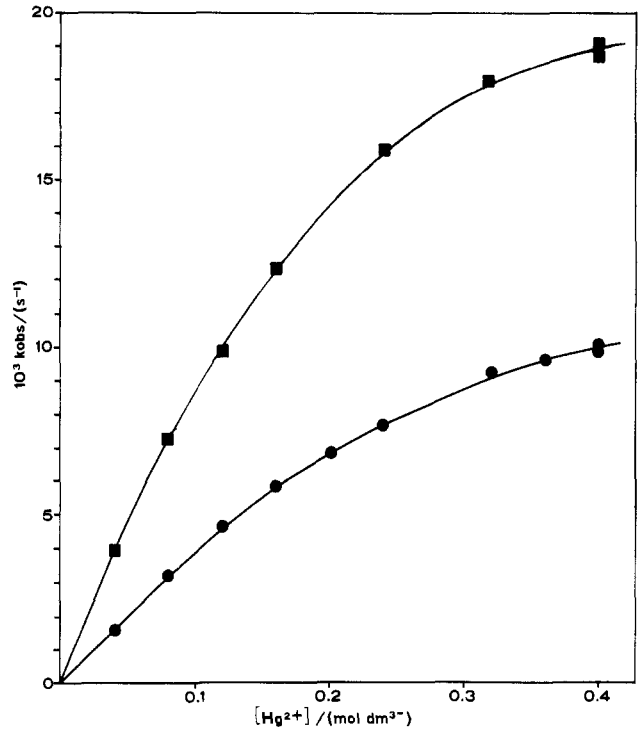

Figure 3. Variation in k_{obsd} with $[Hg^{2+}]$ (0.1–1.36 mol dm^{-3}) at constant I = 1.40 mol dm^{-3}, constant $[H^+]$ = 0.20 mol dm^{-3}, λ = 550 nm, 25.0 °C, and $[Y^-]$ = 1.36–1.00 mol dm^{-3}: (■) NO_3^-; (●) ClO_4^-.

Table I. Kinetic Data for the Ag^+-Catalyzed Reaction of *t*-$[Co(tren)(NH_3)SCN](ClO_4)_2$ in 1.00 mol dm^{-3} ClO_4^- (25.0 °C)

$[Ag^+]$, mol dm^{-3}	$[H^+]$, mol dm^{-3}	10^4k_{obsd}, s^{-1}	$10^4k_{obsd}/[Ag^+]$, mol^{-1} dm^{-3} s^{-1}	10^4k_{calcd},[a] s^{-1}
1.0	0.05	5.0	5.0	5.1
0.75	0.05	3.73	5.0	3.68
0.50	0.05	2.45	4.9	2.25
0.50	0.05	2.40	4.8	2.25
0.50	0.025	2.27	4.5	2.25
0.15	0.025	0.57	3.8	0.57
0.125	0.05	0.47	3.8	0.48

[a] Calculated from (7a) by using K^1_{Ag} = 1.0 mol^{-1} dm^3, k_1 = 3.4 × 10^{-4} s^{-1}, and $k_2K^2_{Ag}$ = 6.8 × 10^{-4} mol^{-1} dm^3 s^{-1}.

straightforward and time efficient. The latter aspect is of some importance when one of the products itself slowly aquates under the conditions (cf. $CoONO_2^{3+}$, see below). Rate data given in Table I were obtained from linear plots of log $[CoSCN^{2+}]$ vs time. It shows an independence of $[H^+]$, and, possibly, a slightly greater than first-order dependence on $[Ag^+]$ (second to last column).

The data of Table I were obtained at $[ClO_4^-]$ = 1.0 mol dm^{-3}, and although the presence of NO_3^- was found to catalyze the reaction, this aspect was not investigated in detail. The reason for this was principally the slowness of the reaction compared to that with Hg^{2+} (viz. $t_{1/2} \approx 20$ min for 0.5 mol dm^{-3} Ag^+ vs 35 s for 0.4 mol dm^{-3} Hg^{2+}, both 1.0 mol dm^{-3} in NO_3^-), and qualitative RP-HPIPC data clearly showed that the $CoONO_2^{2+}$ product undergoes some aquation over the times necessary for complete reaction. Although this does not affect the $CoSCN^{2+}$ data and hence the rate of the initial reaction, it does affect the product distribution. Qualitatively the reaction is accelerated by a factor of about 2 when 1.0 mol dm^{-3} $AgClO_4$ was replaced by 1.0 mol dm^{-3} $AgNO_{3+}$.

2. Reaction Products. (a) Hg^{2+}-Catalyzed Reaction. Three sets of product data were obtained by RP-HPIPC analysis after some 5 reaction half-lives. The first (Table II) shows little variation with increasing $[CF_3SO_3^-]$ (0.10–0.50 mol dm^{-3}) and extrapolates to 58% $CoNCS^{2+}$ and 42% $CoOH_2^{3+}$ at $[CF_3SO_3^-]$ = 0.00 mol dm^{-3}. This distribution corresponds to the Y^--independent pathway (cf. Discussion). Table II also gives products

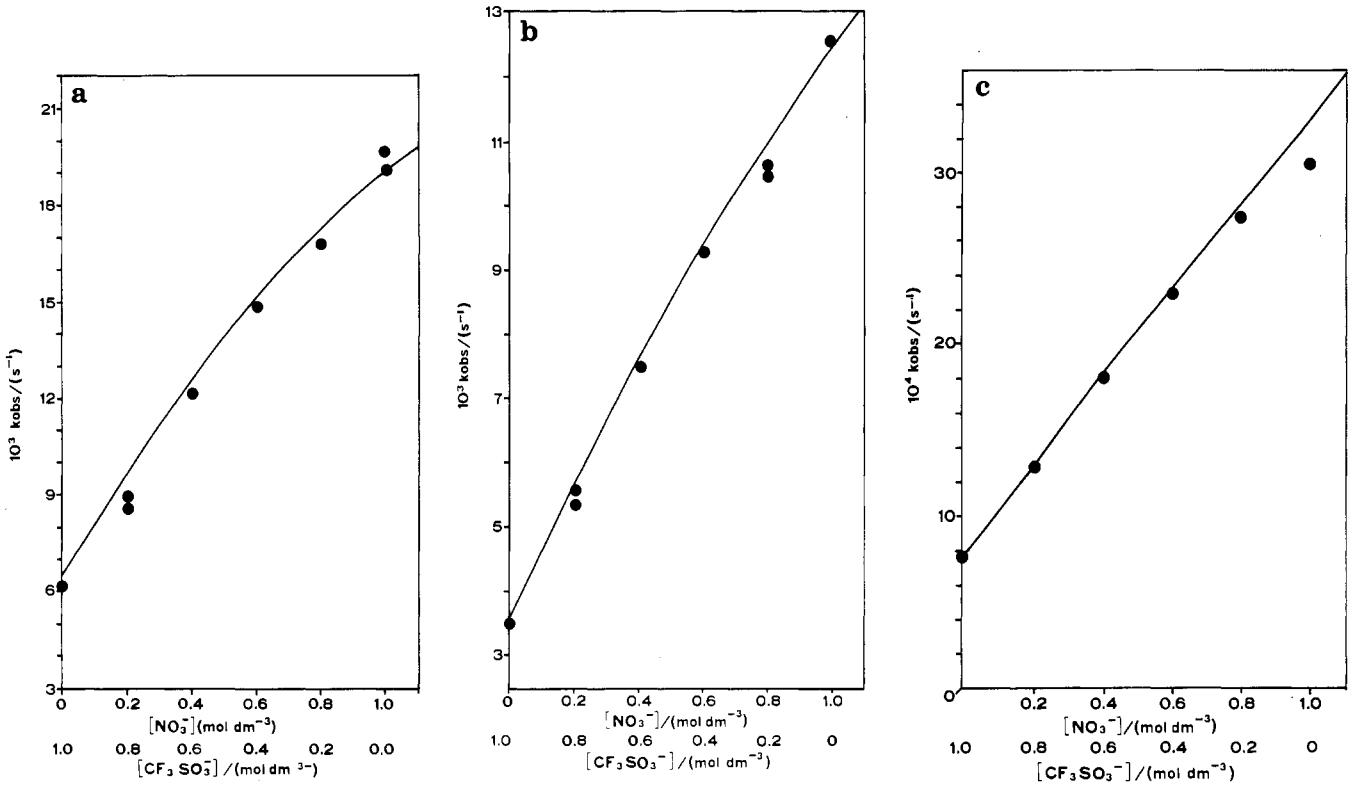

Figure 4. Variations in k_{obsd} using mixed $[NO_3^-] + [CF_3SO_3^-] = 1.00$ mol dm^{-3} solutions at $\lambda = 550$ nm and 25.0 °C. (a) $[Hg^{2+}] = 0.40$, $[H^+] = 0.20$ mol dm^{-3}; (b) $[Hg^{2+}] = 0.20$, $[H^+] = 0.10$ mol dm^{-3}; (c) $[Hg^{2+}] = 0.04$, $[H^+] = 0.02$ mol dm^{-3}.

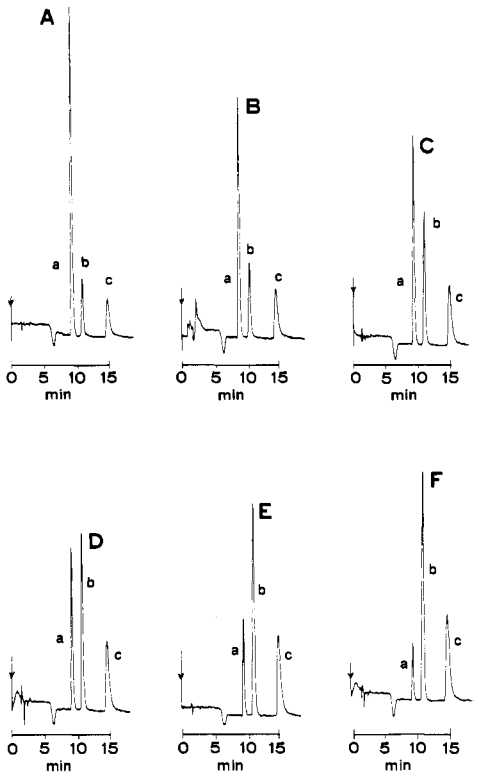

Figure 5. RP-HPIP chromatograms obtained during the reaction with 0.50 mol dm^{-3} $AgClO_4$ at 25.0 °C, $I = 1.00$ mol dm^{-3} ($NaClO_4$), $\lambda = 500$ nm, and AUFS = 0.05, for 20 μL injections. Chromatograms (time in min): A (5), B (23), C (41), D (59), E (93), F (131). Labels a–c refer to the reactants $CoSCN^{2+}$, $CoNCS^{2+}$, and $CoOH_2^{3+}$, respectively.

for various ClO_4^- solutions (variable ionic strength, 1.40–1.04 mol dm^{-3}) and shows the independence of the product distribution on both $[Hg^{2+}]$ and $[H^+]$. The data for 0.5 mol dm^{-3} ClO_4^-, however, differs from that in 1.0 mol dm^{-3} ClO_4^-, being about halfway toward that for the Y^--independent pathway. Clearly the presence

Table II. Products for the Hg^{2+}-Catalyzed Reaction of t-[Co(tren)(NH3)SCN]Br2 in ClO_4^- and $CF_3SO_3^-$ Solutions (25.0 °C)

$[Y^-]$, mol dm^{-3}	$[Hg^{2+}]$, mol dm^{-3}	$[H^+]$, mol dm^{-3}	mol % products[a]	
			$CoNCS^{2+}$	$CoOH_2^{3+}$
		$Y^- = CF_3SO_3^-$		
0.10	0.04	0.02	57.8	42.2
0.10	0.04	0.02	57.2	42.8
0.30	0.04	0.02	56.5	43.5
0.30	0.04	0.02	56.5	43.5
0.50	0.04	0.02	56.0	44.0
0.50	0.04	0.02	56.2	43.8
		$Y^- = ClO_4^-$		
0.5	0.20	0.10	50.1	49.9
1.0	0.04	0.02	42.4	57.6
1.0	0.20	0.20	43.3	56.7
1.0	0.20	0.10	42.0	58.0
1.0	0.40	0.20	42	58

[a] Analyses based on extinction at 500 nm given as footnote *a* to Table III.

Table III. Products[a] for the Hg^{2+}-Catalyzed Reaction of t-[Co(tren)(NH3)SCN]Br2 in NO_3^- Solution ($[Hg^{2+}] = 0.04$ mol dm^{-3}, $[H^+] = 0.02$ mol dm^{-3}; 25.0 °C; I(variable) = 0.14–1.04 mol dm^{-3})

$[NO_3^-]$, mol dm^{-3}	mol % products			$CoNCS^{2+}/CoOH_2^{3+}$
	$CoONO_2^{2+}$	$CoNCS^{2+}$	$CoOH_2^{3+}$	
0.00[b]	0	57.8	42.2	1.38
0.10	31.4	38.9	29.7	1.31
0.20	37.9	34.3	27.9	1.23
0.40	45.6	30.9	23.5	1.31
0.60	49.3	28.6	22.0	1.30
0.80	52.2	26.6	21.2	1.25
1.00	55.5	24.4	20.1	1.21
1.00	54.9	24.7	20.4	1.21

[a] RP-HPIPC analysis at 500 nm using the following molar absorbtivities (mol^{-1} dm^3 cm^{-1}): 129 ($CoONO_2^{2+}$), 156 ($CoSCN^{2+}$), 320 ($CoNCS^{2+}$), 103 ($Co-OH_2^{3+}$). [b] Data from extrapolation of the $CF_3SO_3^-$ data (Table II) to $[CF_3SO_3^-] = 0.00$ mol dm^{-3}.

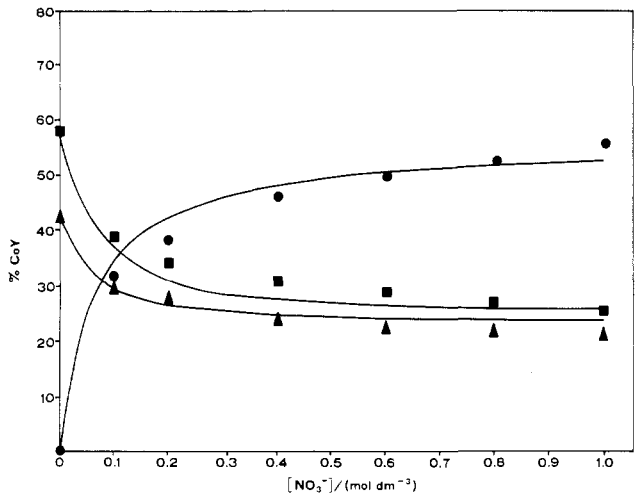

Figure 6. Products of the Hg^{2+}-induced reaction using a variable NO_3^- medium (0.10–1.00 mol dm^{-3}), constant $[Hg^{2+}]$ = 0.04 mol dm^{-3}, and constant $[H^+]$ = 0.02 mol dm^{-3}, at 25.0 °C: (●) $CoONO_2^{2+}$; (■) $CoNCS^{2+}$; (▲) $CoOH_2^{3+}$.

Table IV. Products[a] for the Hg^{2+}-Catalyzed Reaction of *t*-$[Co(tren)(NH_3)SCN]Br_2$ in Mixed NO_3^- and ClO_4^- Solutions ($[NO_3^-] + [ClO_4^-]$ = 1.00 mol dm^{-3}, $[Hg^{2+}]$ = 0.20 mol dm^{-3}, $[H^+]$ = 0.10 mol dm^{-3}; 25.0 °C; I = 1.20 mol dm^{-3})

$[NO_3^-]$, mol dm^{-3}	$[ClO_4^-]$, mol dm^{-3}	mol % products			$CoNCS^{2+}/CoOH_2^{3+}$
		$CoONO_2^{2+}$	$CoNCS^{2+}$	$CoOH_2^{3+}$	
0.0	1.0	0.0	42.0	58.0	0.72
0.1	0.9	11.3	38.7	50.0	0.77
0.2	0.8	20.3	35.6	44.2	0.81
0.4	0.6	32.3	31.8	35.9	0.89
0.6	0.4	41.0	28.4	30.6	0.93
0.8	0.2	49.2	27.1	23.7	1.14
1.0	0.0	52.5	24.2	23.3	1.04
1.0[b]	0.0	51.7	24.2	24.1	1.00

[a] As for Table III. [b] $[Hg^{2+}]$ = 0.10 mol dm^{-3}, $[H^+]$ = 0.05 mol dm^{-3}, I = 1.10 mol dm^{-3}.

of ClO_4^- enhances the amount of $CoOH_2^{3+}$ at the expense of $CoNCS^{2+}$. The second set of data (Table III) was obtained by using the same solutions as those used for the kinetic data of Figure 1, i.e. constant $[Hg^{2+}]$ = 0.04 mol dm^{-3}, constant $[HNO_3]$ = 0.02 mol dm^{-3}, and varying $[NO_3^-]$ = 0.10–1.00 mol dm^{-3}. The data are plotted against $[NO_3^-]$ in Figure 6 and clearly show a limiting distribution for all three products. The $CoNCS^{2+}/CoOH_2^{3+}$ ratio also shows a small but real decrease from 1.38 at $[NO_3^-]$ = 0 to ~1.2 at $[NO_3^-]$ = 1.0 mol dm^{-3}. This means that the presence of NO_3^- decreases $CoNCS^{2+}$ production to a slightly greater extent than it decreases $CoOH_2^{3+}$ production. This is to be compared with the effect of ClO_4^-, $CoNCS^{2+}/CoOH_2^{3+}$ = 0.72 in 1.0 mol dm^{-3} ClO_4^-, which enhances $CoOH_2^{3+}$ at the expense of $CoNCS^{2+}$ (see above). The third set of products (Table IV) relates to the same conditions as those used for the kinetic results of Figure 4; i.e., constant $[NO_3^-] + [ClO_4^-]$ = 1.0 mol dm^{-3}, $[Hg^{2+}]$ = 0.20 mol dm^{-3}, and [HY] = 0.10 mol dm^{-3}. The results are plotted in Figure 7. Once again limiting distributions are being approached at 1.0 mol dm^{-3} NO_3^-, but the trends are now more gradual. At a particular NO_3^- concentration, less $CoONO_2^{2+}$ is produced when ClO_4^- is present than when it is absent (Table III, Figure 6), and the change in $CoNCS^{2+}$ (and $CoOH_2^{3+}$) with increasing $[NO_3^-]$ is less abrupt. The $CoNCS^{2+}/CoOH_2^{3+}$ ratio now increases from 0.72 to ~1.0, showing that replacement of ClO_4^- by NO_3^- results in decreasing amounts of $CoOH_2^{3+}$. This is consistent with the earlier observation that the presence of ClO_4^- favors $CoOH_2^{3+}$ production.

(b) Ag^+-Catalyzed Reaction. Two sets of results were obtained by RP-HPIPC analysis. The first (Table V) corresponds to a constant $[ClO_4^-]$ (1.00 mol dm^{-3}) and variable $[Ag^+]$ (0.125–1.00 mol dm^{-3}) and $[H^+]$ (0.025–0.05 mol dm^{-3}). In contrast to the

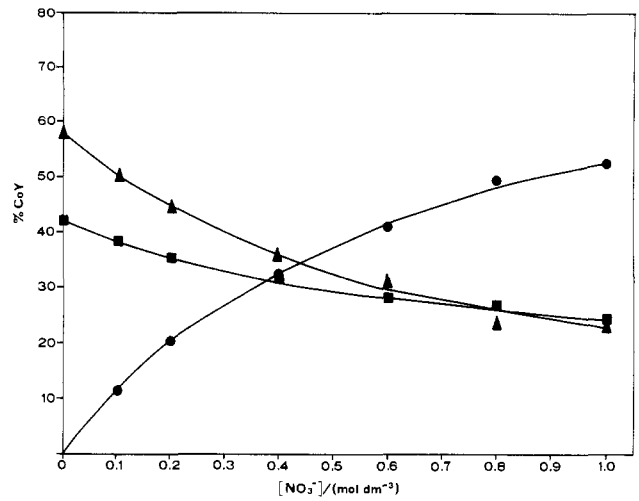

Figure 7. Products of the Hg^{2+}-induced reaction using mixed $[NO_3^-] + [ClO_4^-]$ = 1.00 mol dm^{-3} and constant $[H^+]$ = 0.10 mol dm^{-3} at 25.0 °C: (●) $CoONO_2^{3+}$; (■) $CoNCS^{2+}$; (▲) $CoOH_2^{3+}$.

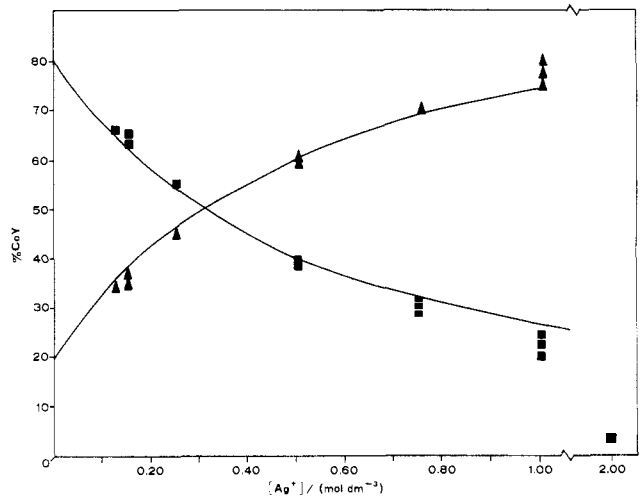

Figure 8. Products of the Ag^+-induced reaction as a function of $[Ag^+]$ at constant $[ClO_4^-]$ = 1.00 mol dm^{-3} and 25.0 °C: (■) $CoNCS^{2+}$; (▲) $CoOHO_2^{3+}$.

Table V. Products[a] for the Ag^+-Catalyzed Reaction of *t*-$[Co(tren)(NH_3)SCN](ClO_4)_2$ in 1.0 mol dm^{-3} ClO_4^- (25.0 °C)

$[Ag^+]$, mol dm^{-3}	$[H^+]$, mol dm^{-3}	mol % products	
		$CoNCS^{2-}$	$Co-OH_2^{3+}$
2.0[c]	0.05	3	97
1.0[b]	0.05	20.0 (6)	80.0 (6)
1.0[b]	0.05	24.1 (4)	75.9 (4)
1.0	0.05	22.5	77.5
0.75	0.0375	30, 31, 28.5	70
0.50[b]	0.05	39 (6)	61 (6)
0.50	0.025	40	60
0.25	0.0235	55	45
0.15[b]	0.05	63 (6)	37 (6)
0.15[b]	0.05	65 (6)	35 (6)
0.125[b]	0.05	66 (6)	34 (6)

[a] RP-HPIPC analysis at 500 nm using molar absorbtivities given in footnote *a* in Table III. [b] Successive analyses during kinetic experiment. Number of determinations in parentheses and average result are given. [c] $[ClO_4^-]$ = 2.0 mol dm^{-3}.

independence shown on $[Hg^{2+}]$ (Table II), the products now show a clear $[Ag^+]$ dependence and this is plotted in Figure 8. Such a plot extrapolates to ~80% $CoNCS^{2+}$ and 20% $CoOH_2^{3+}$ at low $[Ag^+]$ ($CoNCS^{2+}/CoOH_2^{3+} \approx 4.0$), and the results for 2.0 mol dm^{-3} Ag^+ imply that higher $[Ag^+]$ data will probably extrapolate to 100% $CoOH_2^{3+}$. There is no $[H^+]$ dependence in this data. The second set of results (Table VI) corresponds to a constant

Table VI. Products[a] for the Ag^+-Catalyzed Reaction of t-$[Co(tren)(NH_3)SCN](ClO_4)_2$ in Mixed NO_3 and ClO_4^- Solutions ($[NO_3^-] + [ClO_4^-] = 1.0$ mol dm^{-3}, $[H^+] = 0.05$ mol dm^{-3}, $[Ag^+] = 1.0$ mol dm^{-3}; 25.0 °C)

$[NO_3^-]$, mol dm^{-3}	$[ClO_4^-]$, mol dm^{-3}	mol % products			$CoNCS^{2+}/CoOH_2^{3+}$
		$CoONO_2^{3+}$	$CoNCS^{2+}$	$CoOH_2^{3+}$	
0.0	1.0	0	22.5	77.5	0.29
0.0	1.0	0	24.1	75.9	0.32
0.0[b]	1.0	0	20.0 (6)	80.0 (6)	0.25
0.0[c]	1.0	0	38.8	61.2	0.63
0.0[d]	1.0	0	66.0	34.0	1.94
0.1	0.9	16.2	19.1	64.6	0.30
0.1	0.9	14.3	21.4	64.4	0.33
0.2	0.8	25.3	16.7	58.0	0.29
0.4	0.6	47.0	11.7	41.3	0.28
0.6	0.4	58.8	9.1	32.1	0.28
0.8	0.2	61.1	9.8	29.2	0.34
1.0	0.0	61.3	9.5	29.2	0.33

[a] RP-HPIPC analysis at 500 nm using molar absorbtivities given in footnote *a* in Table III. [b] Kinetic runs; values in parentheses gives number of determinations for which the average is given. [c] $[Ag^+] = 0.50$ mol dm^{-3}, $[H^+] = 0.025$ mol dm^{-3}. [d] $[Ag^+] = 0.125$ mol dm^{-3}, $[H^+] = 0.05$ mol dm^{-3}.

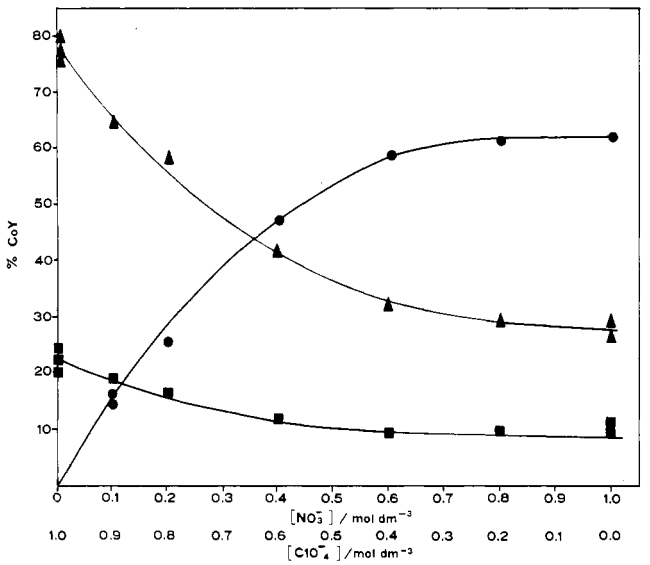

Figure 9. Products of the Ag^+-induced reaction using mixed $[NO_3^-] + [ClO_4^-] = 1.00$ mol dm^{-3} solutions, constant $[Ag^+] = 1.00$ mol dm^{-3}, and constant $[H^+] = 0.05$ mol dm^{-3} at 25.0 °C: (●) $CoONO_2^{3+}$; (■) $CoNCS^{2+}$; (▲) $CoOH_2^{3+}$.

$[Ag^+] = 1.0$ mol dm^{-3} but varying electrolyte (NO_3^-, ClO_4^-) such that $[NO_3^-] + [ClO_4^-] = 1.0$ mol dm^{-3}. The product distributions are plotted against $[NO_3^-]$ in Figure 9, and a saturating condition of ~62% $CoONO_2^{2+}$, 10% $CoNCS^{2+}$, and 28% $CoOH_2^{3+}$ is evident. The $CoNCS^{2+}/CoOH_2^{3+}$ ratio remains essentially constant (0.32 ± 0.02) for varying $NO_3^- + ClO_4^-$ mixtures. It was not practical to investigate the products at lower $[Ag^+]$ because the reaction is then too slow to carry out accurate $CoONO_2^{2+}$ determinations. The products for 1.0 mol dm^{-3} Ag^+ were obtained after about 1 reaction half-life to avoid this problem.

Tracer Experiments in the Presence of $N^{14}CS^-$ and Hg^{2+}. Two experiments were carried out. In the first a t-$[Co(tren)(NH_3)SCN]^{2+}$ solution containing equal amounts of Hg^{2+} and NCS^- (0.033 mol dm^{-3} in each), CF_3SO_3H (0.0167 mol dm^{-3}), and tracer amounts of $N^{14}CS^-$ was warmed at 35 °C. The $CoNCS^{2+}$ product (41% of total) recovered after 4.5 h contained a small but measurable enrichment, 0.7%. The second experiment in the presence of $N^{14}CS^-$ tracer used a somewhat higher concentration of complex ($[Co] = 8.4 \times 10^{-3}$ mol dm^{-3}, $[Hg^{2+}] = [H^+] = [NCS^-] = 0.05$ mol dm^{-3}), and crystals of t-$[Co(tren)(NH_3)SCN]Hg(SCN)_4$ separated after a few minutes. The $CoSCN^{2+}$ in these crystals suggested some enrichment (2.4%), but the larger background and lower concentration of $CoSCN^{2+}$ used in the analytical measurement makes this result uncertain. However when these crystals were heated at 80 °C for 65 h to effect isomerization in the solid state, a large enrichment was realized in the $CoNCS^{2+}$ product, 71%.

Scheme I

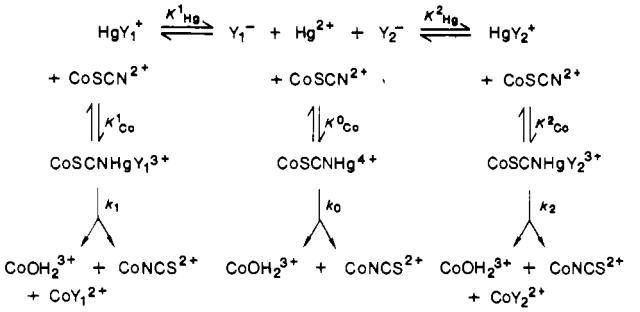

Discussion

1. Treatment of the Hg^{2+} Data. Scheme I sets out our proposal for the mechanism.[23] In aqueous solution Hg^{2+} is involved in equilibria with anions $Y_{1,2}^-$

$$Hg^{2+} + Y_{1,2}^- \overset{K^{1,2}_{Hg}}{\rightleftharpoons} HgY_{1,2}^+ \quad (1)$$

so that

$$[Hg]_T = [Hg^{2+}] + [Co_0] + [Co_1] + [Co_2] + [HgY_1^+] + [HgY_2^+]$$

Since $[Hg]_T \gg [Co]_T$ under our conditions, this becomes

$$[Hg]_T = [H^{2+}] + [HgY_1^+] + [HgY_2^+] = [Hg^{2+}](1 + K^1_{Hg}[Y_1^-] + K^2_{Hg}[Y_2^-]) \quad (2)$$

Similarly

$$[Co]_T = [Co](1 + K^1_{Hg}[Y_1^-] + K^2_{Hg}[Y_2^-] + (K^0_{Co} + K^1_{Co}K^1_{Hg}[Y_1^-] + K^2_{Co}K^2_{Hg}[Y_2^-])[Hg]_T)/(1 + K^1_{Hg}[Y_1^-] + K^2_{Hg}[Y_2^-]) \quad (3)$$

The reaction rate

$$-d[Co]_T/dt = k_0[Co]_0 + k_1[Co]_1 + k_2[Co]_2$$

becomes

$$k_{obsd} = (k_0K^0_{Co} + k_1K^1_{Co}K^1_{Hg}[Y_1^-] + k_2K^2_{Co}K^2_{Hg}[Y_2^-]) \times [Hg]_T/(1 + K^1_{Hg}[Y_1^-] + K^2_{Hg}[Y_2^-] + (K^0_{Co} + K^1_{Co}K^1_{Hg}[Y_1^-] + K^2_{Co}K^2_{Hg}[Y_2^-])[Hg]_T) \quad (4)$$

When only one anion Y_1^- is present, (4) becomes

$$k_{obsd} = (k_0K^0_{Co} + k_1K^1_{Co}K^1_{Hg}[Y_1^-])[Hg]_T/(1 + K^1_{Hg}[Y_1^-] \times (1 + K^1_{Co}[Hg]_T) + K^0_{Co}[Hg]_T) \quad (5)$$

The $[Hg]_T = 0.04$ mol dm^{-3} data, Figure 1, shows a good linear dependence on $[Y_1^-]$ up to at least 1.36 mol dm^{-3} so that $K^1_{Hg}[Y_1^-](1 + K^1_{Co}[Hg]_T)$ must be small unless unusual activity effects are operating. Thus $K^1_{Hg} < 1$, and if K^0_{Co} is also much less than unity, (5) becomes

$$k_{obsd} = 0.04(k_0K^0_{Co} + k_1K^1_{Co}K^1_{Hg}[Y_1^-]) \quad (5a)$$

The data give $k_0K^0_{Co} = 4.3 \times 10^{-3}$ mol^{-1} dm^3 s^{-1} and respective values for $k_1K^1_{Co}K^1_{Hg}$ of 7.1×10^{-2} (NO_3^-), 2.8×10^{-2} (ClO_4^-), and 1.4×10^{-2} ($CF_3SO_3^-$) mol^{-1} dm^3 s^{-1} for this condition. The figure shows a common intercept $k_0K^0_{Co}$ at $[Y_1^-] = 0$ for each Y_1^-; i.e., there is a recognizable pathway to products that is Y^- independent. This pathway decreases in importance with increasing $[Y_1^-]$ but has contributions of 5.6% (NO_3^-), 13.3% (ClO_4^-), and 23% ($CF_3SO_3^-$) at $[Y_1^-] = 1.0$ mol dm^{-3}. This analysis assumes that activity effects are small or that they ef-

fectively cancel. It is likely that these relative contributions remain the same at each $[Hg]_T$ since $K^1_{Hg} < 1$ (eq 5).

The reaction products under the same condition (Table III) can be fitted to (5a) (or to (5)), and the full curves given in Figure 6 shows the agreement for the above constants, assuming the k_0 path gives 58% $CoNCS^{2+}$ and 42% $CoOH_2^{3+}$ (established by the data in Table II) and the k_{NO_3} path gives 55% $CoONO_2^{2+}$, 23% $CoNCS^{2+}$, and 22% $CoOH_2^{3+}$. A somewhat better fit is achieved by using a somewhat larger $k_0K^0_{Co}$ contribution (viz. 6.2×10^{-3} mol^{-1} dm^3 s^{-1}) and a k_{NO_3} path giving 57% $CoONO_2^{2+}$, 23% $CoNCS^{2+}$, and 20% $CoOH_2^{3+}$. However the two sets of values lie within the error of the kinetic and product determinations.

For the kinetic data at constant $[Y^-] = 1.0$ mol dm^{-3} and variable $[Hg]_T$, (5) may be rewritten

$$(k_{obsd})^{-1} = \frac{1 + K^1_{Hg}}{(k_0K^0_{Co} + k_1K^1_{Co}K^1_{Hg})[Hg]_T} + \frac{K^1_{Co}K^1_{Hg} + K^0_{Co}}{k_0K^0_{Co} + k_1K^1_{Co}K^1_{Hg}} \quad (5b)$$

From linear plots of $(k_{obsd})^{-1}$ vs $[Hg]_T^{-1}$, Figure 10 (supplementary material), the intercepts at $[Hg]_T^{-1} = 0$ (24 (NO_3^-), 25 (ClO_4^-), 30 s ($CF_3SO_3^-$)) lead to k_1 values of $(3.9 \pm 0.5) \times 10^{-2}$ (NO_3^-), $(3.5 \pm 0.5) \times 10^{-2}$ (ClO_4^-), and $(2.6 \pm 0.5) \times 10^{-2}$ s^{-1} ($CF_3SO_3^-$). Intercepts for similar plots of the constant ionic strength data of Figure 3 (cf. Figure 11, supplementary material) lead to similar k_1 values for NO_3^- and ClO_4^- (3.6×10^{-2} (NO_3^-), 2.5×10^{-2} s^{-1} (ClO_4^-)). From the slopes of Figure 10 the following $K^1_{Co}K^1_{Hg}$ values result: 2.2 ± 0.3 (NO_3^-), 0.9 ± 0.2 (ClO_4^-), and 0.6 ± 0.1 mol^{-2} dm^6 ($CF_3SO_3^-$).[24] An independent set of $K^1_{Co}K^1_{Hg}$ values (1.7 (NO_3^-), 0.7 (ClO_4^-), 0.4 mol^{-2} dm^6 ($CF_3SO_3^-$)) are obtained by using the above k_1 values and the previous $k_1K^1_{Co}K^1_{Hg}$ values obtained at variable $[Y_1^-]$ and $[Hg]_T = 0.04$ mol dm^{-3}. The two sets are in reasonable agreement.

When both Y_1^- and Y_2^- are present with $[Y_1^-] + [Y_2^-] = 1.00$ mol dm^{-3}, (4) becomes

$$k_{obsd} = (k_0K^0_{Co} + k_2K^2_{Co}K^2_{Hg} + (k_1K^1_{Co}K^1_{Hg} - k_2K^2_{Co}K^2_{Hg})[Y_1^-])[Hg]_T/(1 + K^2_{Hg} + (K^1_{Hg} - K^2_{Hg}) \times [Y_1^-] + (K^2_{Co}K^2_{Hg} + (K^1_{Co}K^1_{Hg} - K^2_{Co}K^2_{Hg})[Y_1^-])[Hg]_T + K^0_{Co}[Hg]_T) \quad (6)$$

which, for $K^{1,2}_{Hg}$ and $K^0_{Co}[Hg]_T < 1$ (see above), becomes

$$k_{obsd} = (k_0K^0_{Co} + k_2K^2_{Co}K^2_{Hg} + (k_1K^1_{Co}K^1_{Hg} - k_2K^2_{Co}K^2_{Hg})[Y_1^-])[Hg]_T/(1 + (K^2_{Co}K^2_{Hg} + (K^1_{Co}K^1_{Hg} - K^2_{Co}K^2_{Hg})[Y_1^-])[Hg]_T) \quad (6a)$$

The full curves of Figure 4 are drawn by using (6a) and the constants found in the presence of the separate Y_1^- anions (viz. $k_0K^0_{Co} = 4.2 \times 10^{-3}$ mol^{-1} s^{-1}, $k_1K^1_{Co}K^1_{Hg} = 1.56 \times 10^{-2}$ mol^{-2} dm^6 s^{-1} ($CF_3SO_3^-$), $k_2K^2_{Co}K^2_{Hg} = 8.50 \times 10^{-2}$ mol^{-2} dm^6 s^{-1} (NO_3^-), $K^1_{Co}K^1_{Hg} = 0.6$ mol^{-2} dm^6 ($CF_3SO_3^-$), and $K^2_{Co}K^2_{Hg} = 2.2$ mol^{-2} dm^6 (NO_3^-)). The agreement with experiment implies that Y_1^- and Y_2^- act independently of each other; i.e., there is no kinetically significant pathway involving Y_1^- and Y_2^- acting in unison.

The reaction products under the conditions $[NO_3^-] + [ClO_4^-] = 1.0$ mol dm^{-3}, $[Hg^{2+}] = 0.20$ mol dm^{-3}, and $[H^+] = 0.10$ mol dm^{-3} can be fitted to (6a) (or to (6)) by using the above kinetic constants and the following product distributions: k_0 path, 58% $CoNCS^{2+}$ and 42% $CoOH_2^{3+}$; k_{NO_3} path, 55% $CoONO_2^{2+}$, 23% $CoNCS^{2+}$, and 22% $CoOH_2^{3+}$; k_{ClO_4} path, 40% $CoNCS^{2+}$ and 60% $CoOH_2^{3+}$. The agreement with experiment is shown by the full curves of Figure 7.

2. Treatment of the Ag^+ Data. Scheme II sets out our proposal for the mechanism. To simplify this treatment the associations of anions $Y_{1,2}^-$ (i.e. ClO_4^-, NO_3^-) with Co_1 and Co_2 have been omitted, but clearly this must occur since CoY^{2+} products are again observed (either directly as $CoONO_2^{3+}$ (Table VI), or indirectly as $CoOClO_3^{2+}$, which subsequently but rapidly aquates to $CoOH_2^{3+}$) in competition with the isomerized product $CoNCS^{2+}$. Anion and H_2O entry is considered to occur via interchange in Co_1Y^{2+}, Co_2Y^{3+}, or $Co_2(Y)_2^{2+}$ species similar to

Scheme II

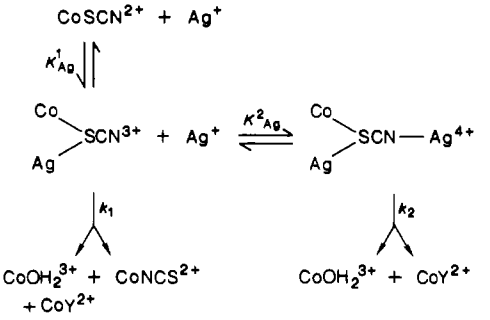

that proposed for the Hg^{2+} reaction. But the absence of detailed kinetic data on the nature of this Y^- involvement together with the limited product data, make the origins of CoY^{2+} less certain for this reaction. Scheme II leads to

$$k_{obsd} = \frac{k_1K^1_{Ag}[Ag^+] + k_2K^1_{Ag}K^2_{Ag}[Ag^+]^2}{1 + K^1_{Ag}[Ag^+] + K^1_{Ag}K^2_{Ag}[Ag^+]^2} \quad (7)$$

which becomes, if $K^2_{Ag} < 1$

$$k_{obsd} = \frac{k_1K^1_{Ag}[Ag^+] + k_2K^1_{Ag}K^2_{Ag}[Ag^+]^2}{1 + K^1_{Ag}[Ag^+]} \quad (7a)$$

The rate data (Table I) clearly show little $[Ag^+]$ dependence above first order, so that $k_2K^2_{Ag} \approx k_1K^1_{Ag}$ and $k_1K^1_{Ag} \approx 5 \times 10^{-4}$ mol^{-1} dm^3 s^{-1}. A more precise fit is achieved by making use of the product data, which extrapolates to ~80% $CoNCS^{2+}$ for the k_1 path and 0% $CoNCS^{2+}$ for the k_2 path (Figure 8). Hence for the $[Ag^+] = 0.5$ mol dm^{-3} result (40% $CoNCS^{2+}$) where the two paths contribute about equally to the rate, we have $k_2K^2_{Ag} = 2k_1$, and for a K^1_{Ag} value of 1.0 mol dm^{-3} (i.e. $k_2K^2_{Ag} = 2k_1K^1_{Ag}$) and a k_1 value of 3.4×10^{-4} s^{-1} a good fit is achieved with the observed rate data (last column of Table I). A fit of the product data with these constants is given by the full curves of Figure 8. Except for the 2.0 mol dm^{-3} Ag^+ result, the agreement is satisfactory.

No analytical significance can be attached to the products in the presence of $[NO_3^-] + [ClO_4^-] = 1.0$ mol dm^{-3} (Figure 9) except that the obvious limiting distributions in 1.0 mol dm^{-3} NO_3^- implies that, compared to the Hg^{2+} data (Figure 7), entry of NO_3^- is relatively more important than entry of ClO_4^-. This is also borne out by the greater constancy in the $CoNCS^{2+}/CoOH_2^{3+}$ ratio, in this case (0.32 ± 0.02), compared to that for the Hg^{2+} reaction (0.72 to ~1.10–1.2) where increasing $CoOH_2^{3+}$ is taken to result from increased $CoOClO_3^{2+}$ involvement (but see point 10 below).

Comparison of Reaction Pathways. A comparison of the rate, equilibrium, and product data for the Hg^{2+} reaction provides some useful observations.

1. The differences in rate reside in differences in the binding of Hg^{2+} and Y^- to $CoSCN^{2+}$. The $K^1_{Co}K^1_{Hg}$ value decreases by about a factor of 2 for each of the anions NO_3^-, ClO_4^-, and $CF_3SO_3^-$ (2.2, 0.9, and 0.6 mol^{-2} dm^6, respectively), and if a somewhat smaller value of 0.1 mol^{-1} dm^3 is taken for the anion-independent association constant K^0_{Co} a value of 4×10^{-2} s^{-1} is obtained for k_0. Since the analysis of the rate data requires $K^1_{Hg} < 1$ the binding of HgY_1^+ to $CoSCN^{2+}$ must be appreciable, $K^1_{Co} > 1$.

2. The k_Y values for each of the anions NO_3^-, ClO_4^- and $CF_3SO_3^-$ are about the same, $(3 \pm 1) \times 10^{-2}$ s^{-1}, implying that Y^- either plays no significant role, or the same role, in the activation process for breaking the $Co–SCN^{2+}$ bond. The estimate for k_0 of 4×10^{-2} s^{-1} suggests that Y^- plays little part, but at this time this aspect cannot be verified.

3. The presence of the internal competitor SCN^- allows a more detailed picture to be drawn as to how the products are formed. The appearance of $CoNCS^{2+}$ in addition to $CoONO_2^{2+}$ and $CoOH_2^{3+}$ suggests that each entering group, NCS^-, ONO_2^-, and OH_2, is in direct competition for the same "Co" intermediate. The suggestion[3] that $CoNCS^{2+}$ is formed by bond rotation at an early

stage in an intermediate such as

and that $CoONO_2^{2+}$ and $CoOH_2^{3+}$ are formed subsequently following diffusion of released SCN^- into the adjoining (or bulk) solvent is untenable. Such a process would predict a constant amount of $CoNCS^{2+}$ irrespective of both the nature and concentration of Y^-; only the $CoY^{2+}/CoOH_2^{3+}$ ratio would vary with the different Y^- and with its concentration if entry were $[Y^-]$ dependent. This is not found. The 58% $CoNCS^{2+}$ produced in the absence of electrolyte, 42% in 1.0 mol dm^{-3} ClO_4^-, and 24% in 1.0 mol dm^{-3} NO_3^- clearly shows that the presence of Y^- significantly affects the formation of the bond-rotated species. The fact that decreased amounts of $CoNCS^{2+}$ are formed as $[Y^-]$ increases suggests a competitive process at the reaction site.

4. The intermediacy in the amount of $CoNCS^{2+}$ formed in a ClO_4^- medium (42% in 1.0 mol dm^{-3}) compared to that in its absence (58%) and that in the presence of 1.0 mol dm^{-3} NO_3^- (24%) infers that ClO_4^- competes for the bond-rotation process but to a lesser extent than NO_3^-. Furthermore, the larger amount of $CoOH_2^{3+}$ formed in a ClO_4^- medium (58%) compared to that in its absence (42%) or to that in 1.0 mol dm^{-3} NO_3^- (23%) suggests either that ClO_4^- in some way encourages OH_2 entry (whereas NO_3^- inhibits it), or that ClO_4^- also enters to give $CoOClO_3^{2+}$, which subsequently aquates (rapidly) to produce $CoOH_2^{3+}$. The former possibility seems unlikely in view of the comparative closeness in the $CoNCS^{2+}/CoOH_2^{3+}$ ratios in the absence of electrolyte and in the presence of NO_3^- (1.38 and 1.15, respectively), compared to that when ClO_4^- is present (0.67). The alternative possibility of direct entry of ClO_4^- to give $CoOClO_3^-$ is given support by the observation that $[Co(NH_3)_5OClO_3]^{2+}$ is detected as a transient intermediate ($t_{1/2}$ for aquation = 7 s) following the more rapid Hg^{2+}-induced removal of halide from $[Co(NH_3)_5Br]^{2+}$ and $[Co(NH_3)_5I]^{2+}$ in ClO_4^- media.[5]

5. The fact that all of the $CoONO_2^{2+}$ product can be accommodated by the k_{NO_3} pathway infers that the activated complexes for breaking the Co–SCN^{2+} bond and for forming the products have the same composition. Furthermore, the juxtaposition of $HgONO_2^+$ and the departing ligand suggests that the kinetically involved NO_3^- is probably that which enters the complex: i.e., the two processes are intimately related in a stereochemical sense, viz.

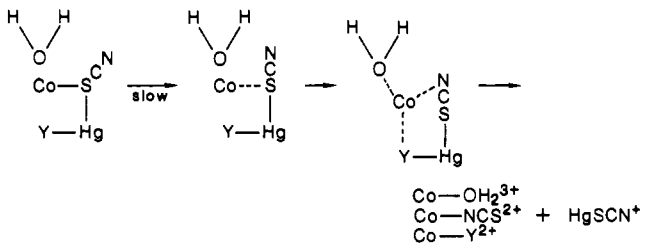

The separately determined product distributions for the anion-independent pathway k_0 (58% $CoNCS^{2+}$, 42% $CoOH_2^{3+}$), the k_{ClO_4} pathway (40% $CoNCS^{2+}$, 60% $CoOH_2^{3+}$), and the k_{NO_3} pathway (23% $CoNCS^{2+}$, 55% $CoONO_2^{2+}$, 22% $CoOH_2^{3+}$) also satisfy the product distributions obtained for reactions where both NO_3^- and ClO_4^- are present together. This implies that the products arise via independent processes; i.e., ClO_4^- does not influence the entry of NO_3^- and vice versa.

6. The small but real difference in the $CoNCS^{2+}/CoOH_2^{3+}$ ratio for the k_0 and k_{NO_3} paths (1.38 vs 1.05) implies that the same intermediate is not involved in the two cases and that NO_3^- competes more effectively for NCS^- entry than for OH_2 entry. Water entry derives from the adjacent solvent, whereas the rotating SCN^- moiety and the entering ONO_2^- ligand probably both derive from attachment to Hg^{2+}. This juxtaposition apparently results in their influencing each others entry to a greater extent than their influence on OH_2 entry from the adjacent solvent structure. Possibly an interchange process, such as has been suggested for the $CoBr^{2+}$ + Cl_2 (and HOCl) reaction,[6] is involved; i.e.

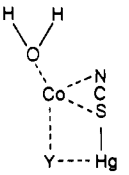

7. The $N^{14}CS^-$ tracer result using equimolar amounts of Hg^{2+} and $N^{14}CS^-$ (0.033 mol dm^{-3}) infers a similar mechanism for self-exchange during the bond-rotation process. The incorporation of 0.7% of $N^{14}CS^-$ is small compared to NO_3^- entry, but $Hg(SCN)_x^{(x-2)-}$ species are much more stable (β_2 = 16.43, β_3 = 19.14, β_4 = 21.12; 0.2 mol dm^{-3} KNO_3, 25 °C)[13] than their $Hg(ONO_2)_x^{(x-2)-}$ counterparts. The low incorporation result probably derives from the comparative preference of Hg^{2+} over Co for SCN^- in an intermediate such as

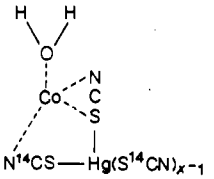

The concentration of unassociated Hg^{2+} in this experiment will be extremely low due to the high stability of $Hg(SCN)_x^{(x-2)-}$, and the products of the reaction almost certainly derive from such a thiocyanate-dependent process. A similar pathway involving $HgCl^+$ has been found in our laboratory for the t-[Co(tren)$(NH_3)Cl]^{2+}$ + Hg^{2+} reaction, and its relative importance is similar to that for $HgONO_2^+$ and $HgOClO_3^+$.[7] It is also possible to interpret the early Posey and Taube results for the [Co$(NH_3)_5Cl]^{2+}$ + Hg^{2+} reaction in the presence of SO_4^{2-} (first and second order in SO_4^{2-} paths were found)[8] in the same manner.

Although less information has been gathered for the Ag^+-induced reaction, some comment here is also possible.

8. The 80% $CoNCS^{2+}$ and 20% $CoOH_2^{3+}$ result for the first order in Ag^+ pathway (in the presence of 1.0 mol dm^{-3} ClO_4^-) differs appreciably from that with Hg^{2+} (42% $CoNCS^{2+}$ and 58% $CoOH_2^{3+}$ under the same conditions). It is unlikely that the difference arises from a major change in the relative k_0 and k_{ClO_4} contributions; it is more likely that it results from differences in the ability of the departing NCSAg and $NCSHg^+$ species to compete with the solvent lattice, and with $OClO_3^-$, for reentry. The relative preference of Co for the nitrogen end of NCSAg compared to $NCSHg^+$ is in keeping with the greater expected basicity of the former and with the influence of Ag^+ in a kinetic sense, which requires AgSCN to be a poorer leaving group from Co than $HgSCN^+$. For the spontaneous reaction in the absence of either Ag^+ or Hg^{2+} an even smaller amount (~5%) of $CoOH_2^{3+}$ is formed.[9] This is an obvious extension of this argument.

9. In the presence of *two* Ag^+ ions little (possibly no) $CoNCS^{2+}$ is formed. This is consistent with the view that the departing entity is now $AgSCNAg^+$ in which nitrogen is now unavailable for entry into the coordination sphere.

(5) Harrowfield, J. MacB.; Sargeson, A. M.; Singh, B.; Sullivan, J. C. *Inorg. Chem.* **1975**, *14*, 2864.
(6) Haim, A.; Taube, H. *J. Am. Chem. Soc.* **1963**, *85*, 3108.
(7) Webley, W. S. Ph.D. Thesis, University of Otago, 1984.
(8) Posey, F. A.; Taube, H. *J. Am. Chem. Soc.* **1957**, *79*, 255.
(9) Buckingham, D. A.; Clark, C. R., unpublished results.
(10) Buckingham, D. A.; Olsen, I. I.; Sargeson, A. M.; Satrapa, H. *Inorg. Chem.* **1967**, *6*, 1027.
(11) Reynolds, W. L.; Alton, E. R. *Inorg. Chem.* **1978**, *17*, 3355.
(12) Jackson, W. G.; Lawrence, G. A.; Sargeson, A. M. *Inorg. Chem.* **1980**, *19*, 1001.
(13) *Stability Constants of Metal-Ion Complexes*; Sillen, L. G., Martell, A. E., Eds.; Chemical Society Special Publication 17; The Chemical Society: London, 1964.

10. The constancy in the $CoNCS^{2+}/CoOH_2^{3+}$ ratio for the various $NO_3^- + ClO_4^-$ mixtures (0.32 ± 0.02, Table VI) suggests either that entry of ClO_4^- is now unimportant compared to NO_3^- entry, with the latter competing equally well for NCS^- and OH_2 entry, or that NO_3^- competes more favorably for the NCS^- pathway with this preference being offset by a decreasing involvement of ClO_4^- to form $CoOClO_3^{2+}$ (which subsequently gives $CoOH_2^{3+}$). We favor the latter interpretation. The constancy in the $CoNCS^{2+}/CoOH_2^{3+}$ ratio also implies that there is no significant change in the relative contributions of the first-order (k_1) and second-order (k_2) Ag^+ pathways with varying electrolyte. These two processes are known to result in different products under the same condition (1.0 mol dm^{-3} $NaClO_4$) so that it is likely these will differ in a NO_3^- medium.

Comparison with Related Induced Reactions. It is likely that the mechanism for the present reaction closely resembles that for the Hg^{2+}-induced removal of halide from $[Co(NH_3)_5Cl]^{2+}$ and $[Co(NH_3)_5Br]^{2+}$. This latter reaction has been extensively studied[8,10,11] and is generally regarded as an excellent example of the S_N1 dissociative process. It also has some relevance to the OH^--induced isomerization of $[Co(NH_3)_5SCN]^{2+}$ where external anions such as N_3^- have been shown to compete only for OH_2 entry, with isomerization to $[Co(NH_3)_5NCS]^{2+}$ occurring at an earlier stage.[14] The following comments are therefore appropriate in the light of the present results.

1. The question[23] as to whether HgY^+ binds to $CoSCN^{2+}$ or whether Hg^{2+} binds first followed by attachment of Y^- to $CoSCNHg^{4+}$ is probably answered by the experiments using $Hg(OAc)_2$ in its reaction with $[Co(NH_3)_5Br]^{2+}$ reported by Jackson, Lawrence, and Sargeson.[12] They found that appreciable quantities of $[Co(NH_3)_5(OCOCH_3)]^{2+}$ were formed in water (or in 1 mol dm^{-3} NO_3^- and ClO_4^-) and argued for the direct process with incorporation of acetate from $Hg(OAc)_2$. A similar role for $HgONO_2^+$ and $HgOClO_3^+$ is likely even though experimental proof will be difficult to obtain.

2. Although a detailed kinetic study has not been reported for the *t*-$[Co(tren)(NH_3)Cl]^{2+} + Hg^{2+}$ reaction, the $CoONO_2^{2+}$ and $CoOH_2^{3+}$ products formed in the presence of NO_3^- show saturation effects with increasing $[NO_3^-]$.[15] The conventional R factor $[CoONO_2^{2+}]/[CoOH_2^{3+}][NO_3^-]$ decreases from 1.09 in 0.1 mol dm^{-3} NO_3^- to 0.92 in 1.0 mol dm^{-3} NO_3^-. A similar decrease was found for the $[Co(NH_3)_5Cl]^{2+} + Hg^{2+}$ reaction (0.96 in 0.15 mol dm^{-3} NO_3^-, 0.83 in 1.0 mol dm^{-3} NO_3^-).[11] For this latter substrate there also seemed to be a close correspondence between the k_{NO_3} kinetic pathway and $CoONO_2^{2+}$ production (even though no evidence for saturation in the rate was reported). Our kinetic studies with *t*-$[Co(tren)(NH_3)Cl]^{2+}$ show clear evidence for a k_{ClO_4} kinetic pathway,[7] and its neglect in the previous study[11] warrants further investigation. Notwithstanding these comments, the larger $[CoONO_2^{2+}]/[CoOH_2^{3+}][NO_3^-]$ ratio found here for the k_{NO_3} pathway (2.07) when compared to that for *t*-$[Co(tren)(NH_3)Cl]^{2+}$ (0.92)[15] implies that the transition states for ONO_2^- and OH_2 entry are different for the two processes, presumably because the leaving group ($HgSCN^+$, $HgCl^+$) still occupies an adjacent site in the solvent cage. Apparently $HgCl^+$ favors OH_2 entry whereas $HgSCN^+$ favors ONO_2^- entry in a comparative sense. Alternatively the argument is that SCN^- bond rotation competes less effectively for ONO_2^- entry than for OH_2 entry, but this possibility seems to be discredited by point 6 in the previous section.

3. The present Ag^+ results reinforce earlier suggestions that the transition states for the formation of products differ in the Ag^+- and Hg^{2+}-induced reactions of $Co(NH_3)_5X^{2+}$ (X = Cl^-, Br^-, I^-). Posey and Taube's $^{18}O/^{16}O$ fractionation data for water entry were different for the two reactions and also showed an anion (NO_3^-, HSO_4^-/SO_4^{2-}) dependence.[16] This was interpreted as the Ag^+ reaction being "partly S_N2" in character with the Hg^{2+} reaction being S_N1. The product results of Dolbear and Taube for the Ag^+-induced process[17] also suggested an unusual NO_3^- dependence when compared to those for the Hg^{2+} reaction.

4. Incorporation of Y^- into the products formed by the nitrosation reaction $CoN_3^{2+} + NOY$ also appears to happen in a different way.[1,2] The absence of a constant amount of CoY^{2+} via this pathway and the formation of substantial amounts of $CoONO_2^{2+}$ when the rate is controlled by NOCl require that CoY^{2+} is not formed via interchange between the substrate and NOY. It has been argued[1] that the products are formed via a subsequent $CoNNO^{2+}\cdot Y^-$ intermediate in which ion-paired Y^- is inherited from the $CoN_3^{2+}\cdot Y^-$ reactant. Alternatively the ion pair with Y^- is formed subsequent to the rate-determining loss of N_2. For the present reaction an intermediate subsequent to the rate-determining step is not required since the products can be accommodated within the rate-determining activated complex.

5. The ability of NO_3^- to compete for the isomerization processes now brings into question the earlier results for the OH^--induced reaction of $Co(NH_3)_5SCN^{2+}$, which was shown to give a constant $CoNCS^{2+}$ result independent of the environment.[14] These results now need careful checking by the RP-HPIPC method.

Solid-State Exchange in *t*-$[Co(tren)(NH_3)SCN][Hg(S^{14}CN)_4)]$. The 71% exchange of $S^{14}CN^-$ into the $CoNCS^{2+}$ product when crystals of this complex are heated at 80 °C clearly shows that thiocyanate bound to Hg^{2+} competes appreciably for the bond-rotation process in the solid state. The difference from the aqueous solution experiment (~0.7%) presumably lies in lattice considerations, although the temperature difference may also contribute. Similar heating of $[Co(NH_3)_5SCN](S^{14}CN)_2$ is known to result in 45% incorporation of label,[18] although heating crystalline $[Co(NH_3)_5SCN]Cl_2\cdot H_2O$ results in only $[Co(NH_3)_5NCS]Cl_2$.[19]

Experimental Section

t-$[Co(tren)(NH_3)SCN]Br_2$ and *t*-$[Co(tren)(NH_3)NCS]Cl_2\cdot 0.5H_2O$ were prepared as reported previously.[20] The former complex was converted to the ClO_4^- salt by passing a concentrated aqueous solution down a Dowex-1 (ClO_4^-) column, quickly reducing the eluted volume to almost dryness, and adding $LiClO_4$ and then MeOH. RP-HPLC analyses of this material showed the presence of a 7.7–7.5% $CoNCS^{2+}$ impurity. A similar analysis of the Br^- salt showed no detectable $CoNCS^{2+}$ impurity (<0.5%). The Hg^{2+}-catalyzed reactions used the Br^- salt, and the Ag^+ reactions used the ClO_4^- salt.

Kinetics. For the Hg^{2+}-catalyzed reaction, rate data were collected by using a Cary 219 spectrophotometer thermostated at 25.0 °C. The complex, dissolved in a little Me_2SO to give a very concentrated solution, was injected (10 μL) into a 1-cm cuvette containing the reaction medium at 25.0 °C, which was quickly shaken and returned to the cell holder. Absorbance data were collected at 550 nm using the 0.1 OD range, and log ($OD_t - OD_\infty$) vs time data were plotted manually.

Rate data for the Ag^+ reaction were collected by RP-HPIPC as detailed below. Constant injections (10–70 μL) were used and the area (A_t) of the $CoSCN^{2+}$ reactant peak was used in log A_t vs time plots.

Reaction Products. Products for both the Hg^{2+}- and Ag^+-induced reactions were determined by RP-HPIPC (reversed-phase–high-performance ion-pair chromatography)[21] analyses using a Radial-Pak C_{18}

(14) Buckingham, D. A.; Creaser, I. I.; Sargeson, A. M. *Inorg. Chem.* **1970**, *9*, 655.
(15) Buckingham, D. A.; Clark, C. R.; Webley, W. S. *J. Chem. Soc., Dalton Trans.* **1980**, 2255.
(16) Posey, F. A.; Taube, H. *J. Am. Chem. Soc.* **1957**, *79*, 255.
(17) Dolbear, G. E.; Taube, H. *Inorg. Chem.* **1967**, *6*, 60.
(18) Thomas, R. J.; Snow, M. R. *Aust. J. Chem.* **1974**, *27*, 1391.
(19) Snow, M. R.; Boomsa, R. *Acta Crystallogr., Sect. B: Struct. Crystallogr. Cryst. Chem.* **1972**, *B28*, 1908.
(20) Gaudin, M. J.; Clark, C. R.; Buckingham, D. A. *Inorg. Chem.* **1986**, *25*, 2569.
(21) Buckingham, D. A. *J. Chromatogr.* **1984**, *313*, 93.
(22) The formulations NCS^- and SCN^- are intended to infer subsequent bonding to Co of the N and S ends of this ion respectively.
(23) An alternative scheme involving the association of Hg^{2+} with $CoSCN^{2+}$ (K^0_{Co}) and subsequent association of Co_0 with $Y_{1,2}^-$ to form $Co_{1,2}$ will also obviously fit the data. A choice between the two schemes clearly cannot be made from experiments reported here (but see Discussion) and in any case is immaterial to the identification of the rate-determining step and means of forming the products. However, since Y^- anions are known to associate reasonably strongly with Cd^{2+} and Ag^+ in aqueous solution,[4] the direct use of $HgY_{1,2}^+$ and $AgY_{1,2}$ has been used in this discussion. A similar choice was made previously with the NOCl-induced reaction of CoN_3^{2+}.[1]

cartridge (10 μm, 100 × 5 mm) in a radial compression Z-module (Waters Assoc.), a Varian 5000 pump, a Waters U6K injector assembly, a thermostated Varian UV-50 variable wavelength detector, and a HP3390A integrator in conjunction with a Varian 9176 recorder. The following solvent and elution program was used: 25 mM *p*-toluenesulfonate at pH 3.5 in water (A) and 95% methanol (B). Time (min), % B: 0, 10; 15, 30; 20, 30. Molar absorbtivities (ϵ, mol^{-1} dm^3 cm^{-1}) at 500 nm were as follows: $CoONO_2^{2+}$, 129; $CoSCN^{2+}$, 156; $CoNCS^{2+}$, 320; $CoOH_2^{3+}$, 103. A linear (Beer's law) response was demonstrated for appropriate mixtures of the pure complexes over the concentration ranges used.

The following reactions were carried out. For the Hg^{2+} experiments 2–5 mg of *t*-[Co(tren)(NH_3)SCN]Br_2 was accurately weighed out and dissolved in 200 μL of the desired electrolyte (0–1.00 mol dm^{-3} $NaClO_4$, $NaCF_3SO_3$, or $NaNO_3$ or distilled water) and 200 μL of the desired Hg^{2+} solution (0.08, 0.4 mol dm^{-3}) in HY (0.04, 0.20 mol dm^{-3}) in the same electrolyte added. After 6–10 reaction half-lives at 25.0 °C (thermostat bath) an appropriate volume (10–80 μL) of 1.0 mol dm^{-3} Na_2SO_4 solution was added, the solution filtered through a micro filter, and the filtrate stored in ice prior to injection onto the HPLC. This was normally within 10 min of quenching.

For the Ag^+ experiments similar quantities (3–5 mg) of *t*-[Co(tren)(NH_3)SCN]$(ClO_4)_2$ were dissolved in 200 μL of mixed 1.0 mol dm^{-3} $AgClO_4$–$NaClO_4$ or $AgClO_4$–$AgNO_3$ solutions (0.05 mol dm^{-3} in $HClO_4$ or HNO_3) and thermostated (25.0 °C) for various times. For the $AgClO_4$–$NaClO_4$ experiments this time was 5–10 $t_{1/2}$; for the $AgClO_4$–$AgNO_3$ experiments this was 1–3 $t_{1/2}$. At high [Ag^+] (0.5–1.0 mol dm^{-3}) the reaction mixture was then diluted with either 100 or 200 μL of water. An appropriate volume of 1.0 or 0.1 mol dm^{-3} NaCl solution was then added, AgCl removed by microfiltration, and the filtrate stored in ice before injection.

$N^{14}CS^-$ Tracer Experiments. To a mixture of 0.50 cm^3 of 0.2 mol dm^{-3} $Hg(CF_3SO_3)_2$ in 0.10 mol dm^{-3} CF_3SO_3H, 1.00 cm^3 of H_2O, 0.50 cm^3 of labeled $KS^{14}CN$ containing 25 × 10^{-6} Ci $KS^{14}CN$ (56.26 Ci mol^{-1}), and 0.50 cm^3 of 0.2 mol dm^{-3} KSCN (unlabeled) at 30 °C was added 4.49 mg of *t*-[Co(tren)(NH_3)SCN]Br_2 dissolved in 0.5 cm^3 of H_2O, and the mixture was warmed at 35 ± 2 °C for 4.5 h. The color of the solution gradually changed from red-purple to red-orange with a half-time estimated as ~0.5 h. A 50-μL aliquot of this solution was diluted with water to 500 cm^3 for counting purposes (1.0 cm^3 of this solution gave 1524 cpm above background, which corresponds to a total $S^{14}CN^-$ enrichment of 4.57 × 10^{11} cpm/mol of SCN^-). The remainder of the solution was diluted to ~50 cm^3 with water and sorbed onto SP-C25 Sephadex ion-exchange resin (10 cm × 1 cm column) and washed with two lots of 500 cm^3 volumes of 0.015 mol dm^{-3} KSCN and then eluted with 0.25 mol dm^{-3} HCl. Counting of the preband eluent (1 cm^3) gave 52 cpm above background (78 vs 26 cpm) so that rotary evaporated residue was reloaded on to fresh SP-C25 resin in a new column, again washed with 100 cm^3 of 0.2 mol dm^3 KSCN, and eluted with 0.25 mol dm^{-3} HCl. Preband counts (1 cm^3) were now 8 cpm above background (42.2 vs 33.6 cpm). The evaporated residue was dissolved in 5.00 cm^3 H_2O and filtered, and the $CoNCS^{2+}$ concentration measured spectrophotometrically (8.19 × 10^{-4} mol dm^{-3}; i.e. 4.095 μmol $CoNCS^{2+}$ in 5.0 cm^3). Counting 1.00 cm^3 of this solution gave 1507 cpm above background (1541 vs 34 cpm), and a repeat measurement after 3 days on a refiltered solution gave 502 cpm for 0.25 cm^3 against a background count of 34.5 cpm. These values correspond to enrichments of 1.839 × 10^9 and 2.280 × 10^9 cpm/mol of $CoNCS^{2+}$, respectively. Allowing for a quenching factor of 0.68 for $CoNCS^{2+}$ (see below), these correspond to incorporations of 0.59% and 0.73% of $N^{14}CS^-$ from the solvent.

In another experiment 3.75 mg of *t*-[Co(tren)(NH_3)SCN]Br_2 dissolved in 0.50 cm^3 of the labeled $KS^{14}CN$ solution was added to unlabled $KSCN^-$ (0.25 cm^3 of 0.2 mol dm^{-3}) and $Hg(CF_3SO_3)_2$ solution (0.25 cm^3, 0.2 mol dm^{-3} CF_3SO_3H) added dropwise at ~40 °C. After a few minutes dark crystals began to separate. (In a separate experiment using unlabeled SCN^-, these were shown to be *t*-[Co(tren)(NH_3)SCN]Hg$(SCN)_4$.) Anal. Calcd: C, 18.63; N, 19.19. Found: C, 18.9; N, 19.0. After 15 min the crystals were removed and washed with aqueous methanol. They were then divided into two portions. The first was dissolved in warm water and loaded onto SP-C25 ion-exchange resin, and the $CoSCN^{2+}$ band was washed and eluted as described above. RP-HPIPC separation of the $CoSCN^{2+}$ product and counting showed enrichment above background (231 vs 64 cpm, for 1.00 cm^3 of a 1.98 × 10^{-5} mol dm^{-3} solution). This corresponds to 1.17 × 10^{10} cpm/mol of $CoSCN^{2+}$. The second portion of crystals was heated at 80 °C for 65 h during which time they changed from red-purple to orange-brown. These were dissolved in 80 cm^3 of warm water containing 2 drops of concentrated HCl and filtered, and a 20-μL sample (made up to 1.0 cm^3) was counted (4241 cpm above background, corresponding to 1.70 × 10^7 cpm in the 80 cm^3 of solution). RP-HPIPC analysis gave the total Co concentration of this solution to be 4.34 × 10^{-4} mol dm^{-3}; thus, there are 4.19 × 10^{11} cpm/mol of Co present. The $CoNCS^{2+}$ band eluted from the RP-HPIPC column (9.8 cm^3) contained 328 nmol of complex and some 7.634 × 10^4 cpm above background (7789 cpm for 1.0 cm^3). Thus the $CoNCS^{2+}$ sample contained 2.33 × 10^{11} cpm/mol, and for a quenching factor of 0.68 (see below), this corresponds to 71% exchange with lattice $N^{14}CS^-$ on heating. Before heating the isolated $CoSCN^{2+}$ product contained (1.17 × 10^{10})(4.9 × 10^{11})$^{-1}$ 100, or 2.4% of the label.

To test for quenching by Co some fully labeled *t*-[Co(tren)$(NH_3)N^{14}CS]Cl_2$ was prepared. To 93.76 mg of *t*-[Co(tren) $(NH_3)(OH_2)](ClO_4)(NO_3)_2$ were added KNCS (0.2 mol dm^{-3} 1.0 cm^3) and 0.35 cm^3 of the above-labeled $KS^{14}CN$ solution. This was heated and taken to dryness several times (steam bath), then loaded onto Dowex 50WX2 ion-exchange resin (H^+ form), washed liberally with dilute HCl, and finally eluted with 2 mol dm^{-3} HCl and taken to dryness. The product was twice recrystallized from water by adding concentrated HCl and then washed with a little MeOH and dried on the filter. A 0.97-mg sample of this material was dissolved in 500 cm^3 of H_2O of which 1.0 cm^3 was counted (10560 counts in 20 min) giving 456 cpm above background. Another sample (90 μg of complex in 1.0 cm^3 of H_2O) gave 454 036 counts in 20 min, or 22 620 cpm above background. These values are to be compared with expected counts of 651 cpm and 34 273 respectively, giving quenching factors of 0.70 and 0.66.

Counting Method. To Bray's scintillation fluid (9.0 cm^3) was added 1.0 cm^3 of the sample solution in a previously unused scintillation vial, and the sample was counted by using a LKB 1217 Rackbeta liquid scintillation counter. Bray's scintillation fluid was prepared by dissolving naphthalene (30 g) and 2,5-diphenyloxazol (2 g) in dioxane. Dry methanol (50 cm^3) and ethylene glycol (10 cm^3) were added, and the volume was made up to 500 cm^3 with dioxane. All reagents were distilled or recrystallized before use.

(24) This analysis assumes that the $k_0K^0_{Co}$ contribution to the $k_0K^0_{Co} + k_1K^1_{Co}K^1_{Hg}$ term of eq 5b has the same relative importance as that found at $[Hg]_T$ = 0.04 mol dm^{-3} and variable [Y^-] and that K^0_{Co} is small relative to $K^1_{Co}K^1_{Hg}$. The latter assumption appears to be justified by consideration of the slope to intercept ratio $(1 + K^1_{Hg})/(K^1_{Co}K^1_{Hg} + K^0_{Co})$, which takes values of 0.38 ($Y^- = NO_3^-$), 0.60 (ClO_4^-), and 1.8 ($CF_3SO_3^-$). In the situation where K^0_{Co} is greater than $K^1_{Co}K^1_{Hg}$, this ratio would be expected to decrease (rather than increase as observed) on substituting $CF_3SO_3^-$ or ClO_4^- for the NO_3^- anion. This arises because K^1_{Hg} is likely to be larger for $Y^- = NO_3^-$ than for $Y^- = ClO_4^-$ or $CF_3SO_3^-$ and because the value of K^0_{Co} will be independent of anion.

Registry No. *t*-[Co(tren)(NH_3)SCN]$^{2+}$, 94423-38-8; Hg, 7439-97-6; Ag, 7440-22-4; NO_3^-, 14797-55-8; ClO_4^-, 14797-73-0; $CF_3SO_3^-$, 37181-39-8.

Supplementary Material Available: Plots of k_{obsd}^{-1} vs $[Hg]_T^{-1}$ given as Figure 10 ((a) NO_3^-; (b) ClO_4^-; (c) $CF_3SO_3^-$) for variable ionic strength data and as Figure 11 (NO_3^-, ClO_4^-) for I = 1.0 mol dm^{-3} data (4 pages). Ordering information is given on any current masthead page.